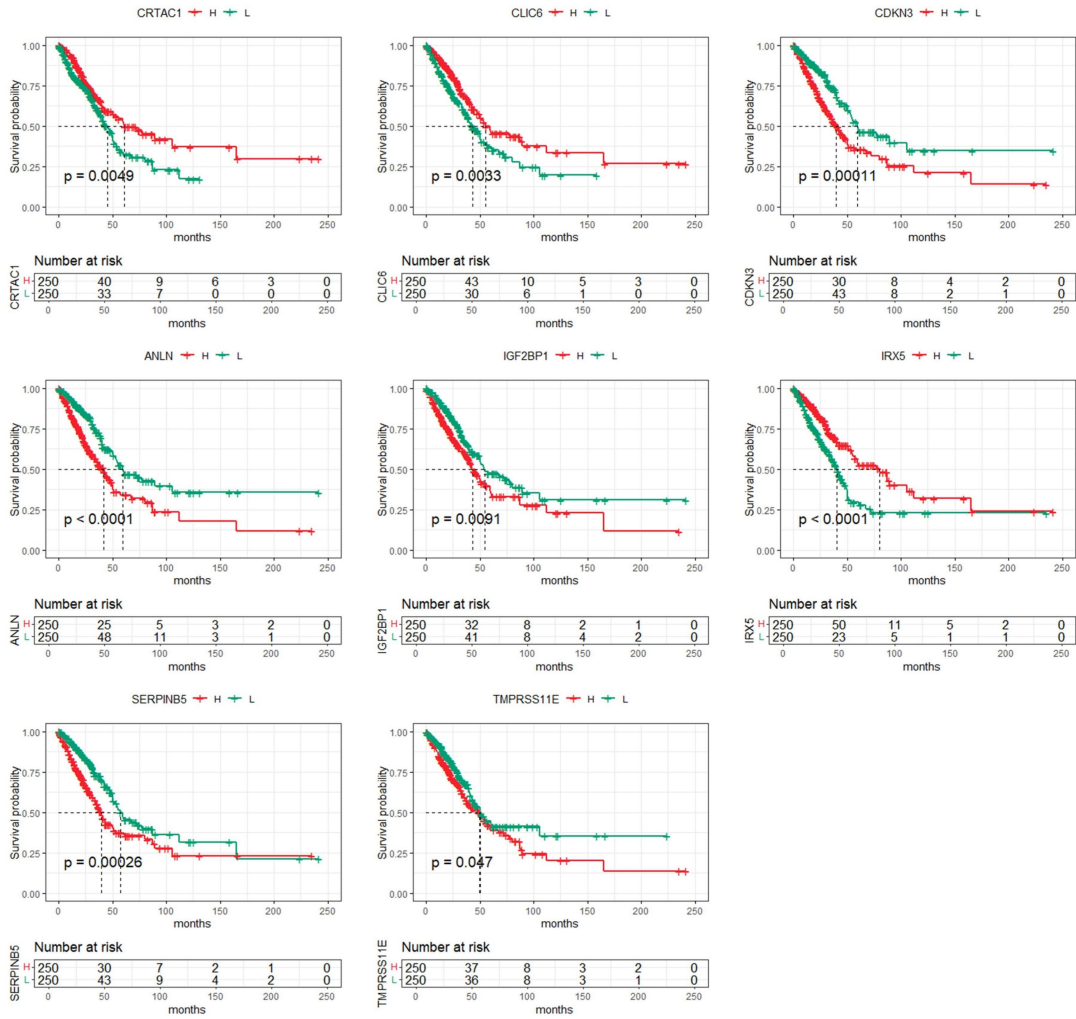
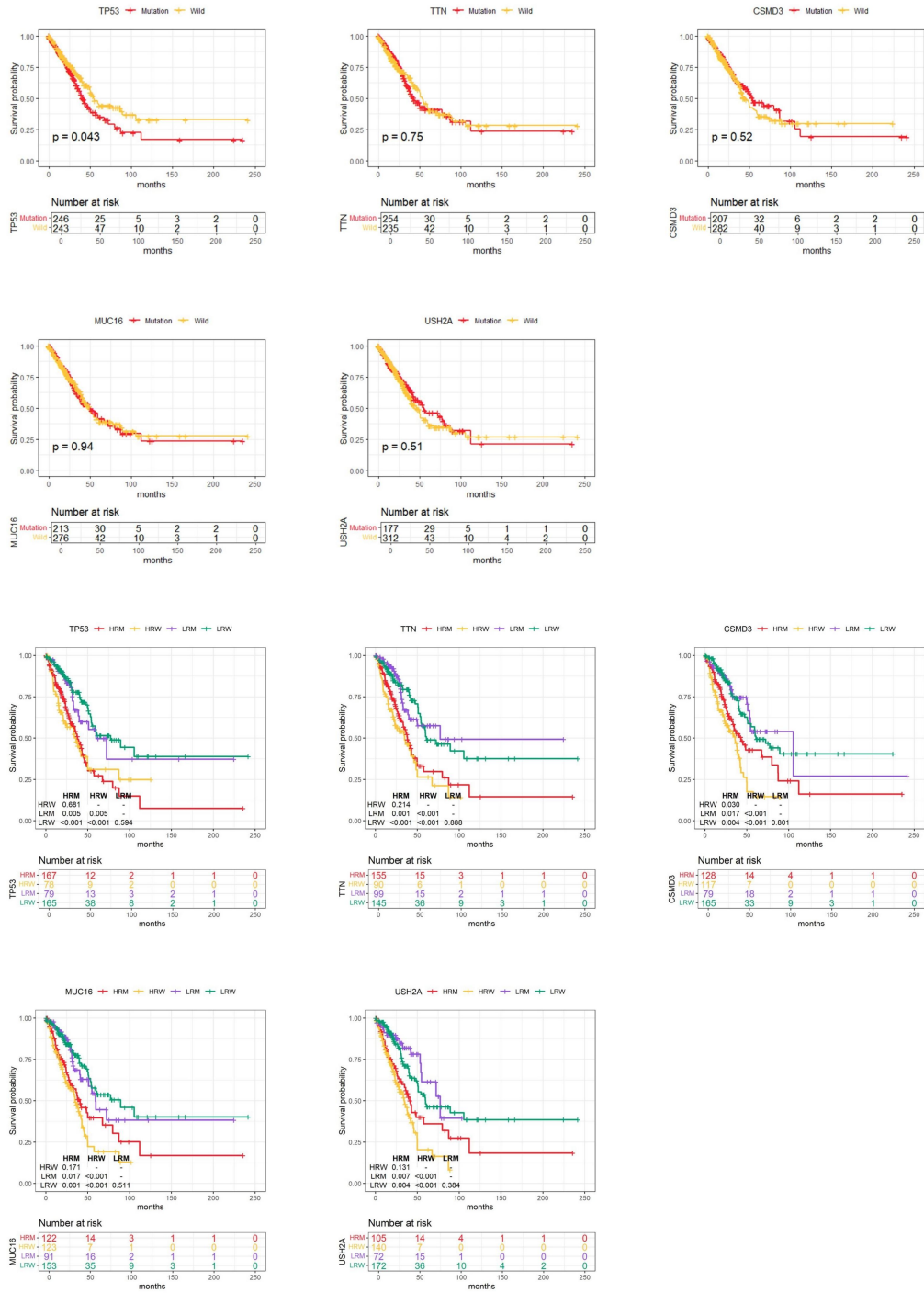


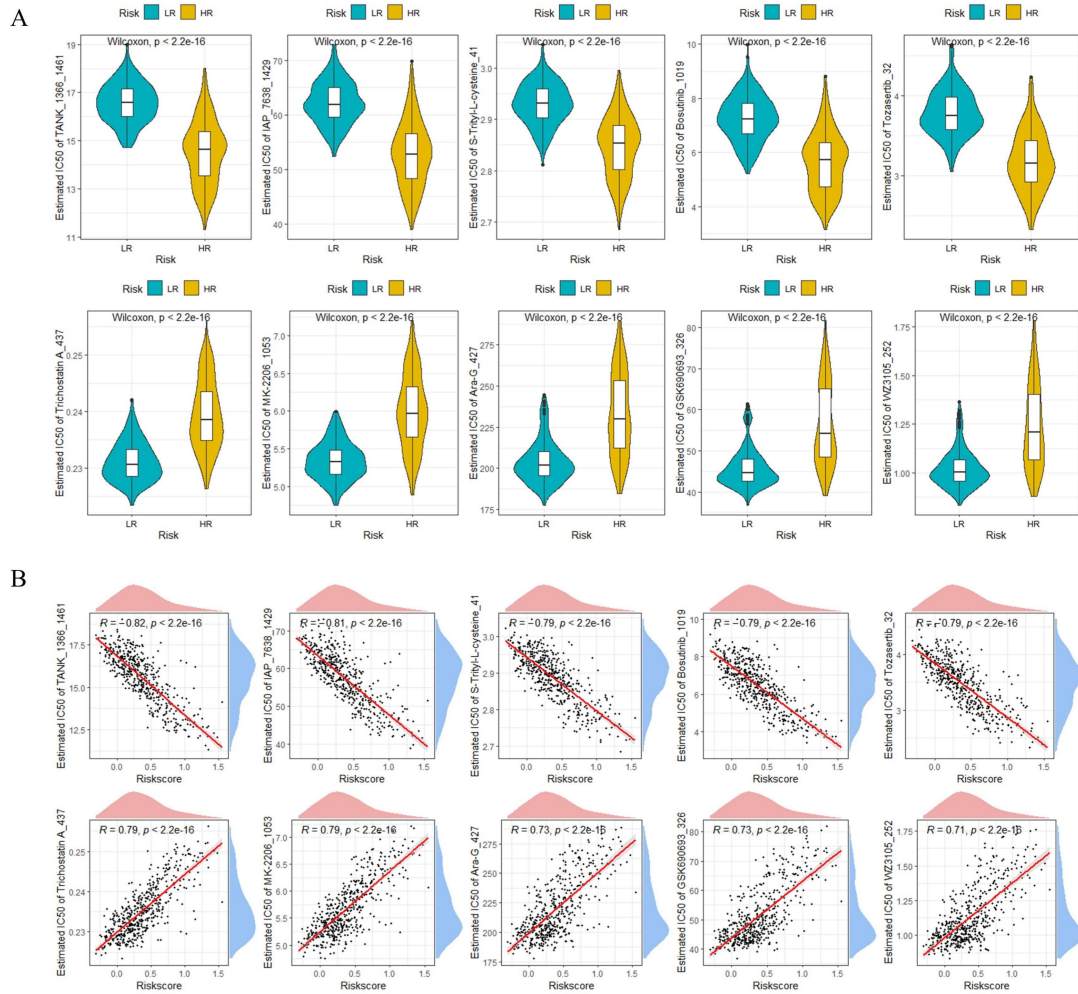
**Supplementary Figure S1. Unsupervised clustering of LUAD samples.** (A) Unsupervised consensus clustering matrix when  $k = 1 - 9$ . (B) Consensus CDF curves showing minimal fluctuations at different consensus indexes. (C) Selection of the optimal clustering number. (D) Trace plot illustrating the clustering of each sample when  $k$  values were set from 2 to 9.



**Supplementary Figure S2.** KM survival curves for each individual signature gene, comparing OS between high and low expression groups.

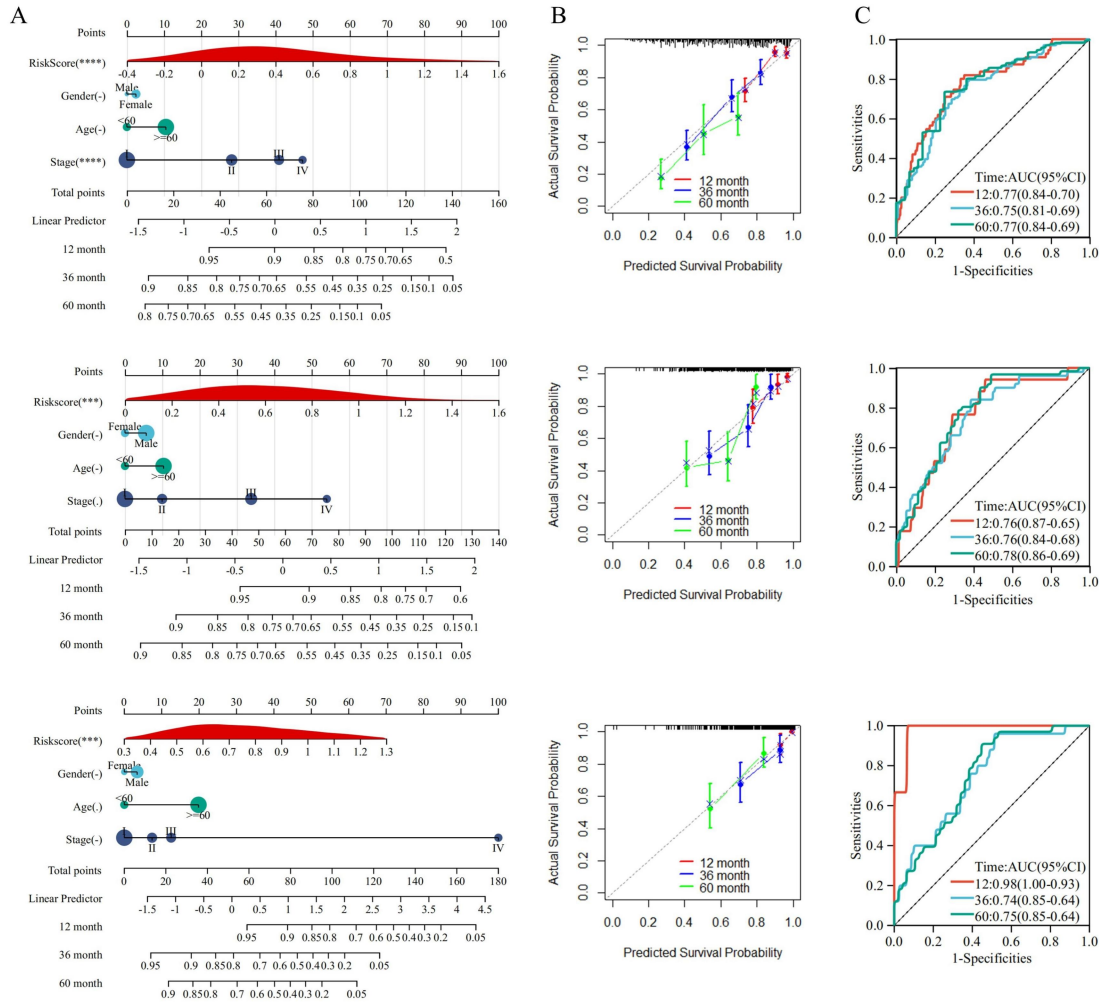


**Supplementary Figure S3. Survival analyses of top mutated genes stratified by mutation status and risk subgroups.** Kaplan-Meier curves for overall survival comparing mutation vs. wild-type status and four risk-mutation subgroups (HRM, HRW, LRM, LRW) for the top five mutated genes (TP53, TTN, CSMD3, MUC16, USH2A). Log-rank test *P*-values and number-at-risk tables are provided for each comparison.



**Supplementary Figure S4.** (A) Violin plots demonstrating significant IC50 differences of top 5 correlated drugs between LR and HR groups. (B) Scatter plots verifying strong correlations ( $|r| > 0.7$ ,  $P < 0.001$ ) between drug IC50 and RiskScore for top 5 correlated agents. \* $P < 0.05$ ; \*\* $P < 0.01$ ; \*\*\* $P < 0.001$ ; ns, not significant.





**Supplementary Figure S6. RiskScore-Based Prognostic Nomogram for LUAD: Calibration and Discrimination Across Cohorts.** (A) Nomograms integrating RiskScore, clinical stage, age, and gender to predict 12-, 36-, and 60-month survival probabilities for TCGA-LUAD, GSE41271, and GSE42127 datasets. (B) Calibration curves comparing predicted and actual survival probabilities at 12, 36, and 60 months across datasets. (C) Time-dependent ROC curves evaluating the model's predictive accuracy for 12-, 36-, and 60-month overall survival. \* $P < 0.05$ ; \*\* $P < 0.01$ ; \*\*\* $P < 0.001$ ; ns, not significant.